15th World Congress on Computational Mechanics (WCCM-XV)
8th Asian Pacific Congress on Computational Mechanics (APCOM-VIII)
Virtual Congress: 31 July – 5 August 2022
S. Koshizuka (Ed.)

MULTI-REGION AND MULTI-COMPONENT THERMAL FLUID ANALYSIS OF HYDROTHERMAL OXIDATIVE DECOMPOSITION REACTOR

HIROYUKI KURAMAE[1], TOKIHIRO SUGIMOTO[2], MASAHIDE MATSUMOTO[3] AND NOBUHISA WATANABE[4]

[1] Osaka Institute of Technology
1-45 Chayamachi, Kita-ku, Osaka 530-8568, Japan
hiroyuki.kuramae@oit.ac.jp, http://www.oit.ac.jp/

[2] Graduate School of Osaka Institute of Technology
1-45 Chayamachi, Kita-ku, Osaka 530-8568, Japan
m1m20r14@st.oit.ac.jp, http://www.oit.ac.jp/

[3] Osaka Institute of Technology
5-1-16 Omiya, Asahi-ku, Osaka 535-8585, Japan
masahide.matsumoto@oit.ac.jp, http://www.oit.ac.jp/

[4] Osaka Institute of Technology
5-1-16 Omiya, Asahi-ku, Osaka 535-8585, Japan
nobuhisa.watanabe@oit.ac.jp, http://www.oit.ac.jp/

Key words: Polychlorinated Biphenyl, Hydrothermal Destruction Reactor, Multi-Region Analysis, OpenFOAM

Abstract. *To elucidate the corrosion mechanism of a hydrothermal oxidation decomposition reactor for the treatment of polychlorinated biphenyls (PCBs), a coupled thermal fluid analysis of the heat transfer between two mixtures of fluids with different physical properties and the reactor body was executed using OpenFOAM. Based on the analysis results, we propose a method to evaluate the corrosion risk at the solid-liquid interface by focusing on three factors: (1) the corrosion temperature of reactor vessel, (2) the amount of fluid deposition that causes corrosion, and (3) the wall shear stress on the solid-liquid interface. Variation of corrosion risk with operating conditions of the reactor is discussed.*

1 INTRODUCTION

Hydrothermal oxidative decomposition is one of methods for detoxification of polychlorinated biphenyls (PCBs, $C_{12}H_{(10-n)}Cl_n$, $1 \leq n \leq 10$), which are decomposed into water (H_2O), carbon dioxide (CO_2) and sodium chloride (NaCl) by dechlorination with sodium carbonate (Na_2CO_3) and oxidative decomposition with liquid oxygen (O_2) under high temperature 370 °C and high pressure 26.5 MPa [2] as follows:

$$2NaOH + CO_2 \longrightarrow Na_2CO_3 + H_2O \tag{1}$$

$$58C_{12}H_{(10-n)}Cl_n + 29nNa_2CO_3 + 19nH_2O \longrightarrow (58-2n)C_{12}H_{10} + 58nNaCl + 53nCO_2 \tag{2}$$

$$29O_2 + 2C_{12}H_{10} \longrightarrow 24CO_2 + 10H_2O \tag{3}$$

In these reactor vessels, wall thinning due to corrosion was observed on bottom inner wall. At present, the reactors have been safely maintained and operated by adding a bottom partition to prevent chemical sinking and supplying hot water to the reactor vessel bottom to control the temperature. Thermal fluid analysis of the hydrothermal oxidative destruction reactors is necessary to clarify the corrosion mechanism.

The authors have been performed multi-regionally coupled analysis of thermal fluid for the internal fluid and heat conduction analysis for the vessel body for hydrothermal oxidative destruction reactor of PCBs [1]. However, this analysis was for a single fluid, water only. Therefore, a finite volume analysis (FVA) solver chtMultiRegionTwoPhaseEulerFoam of OpenFOAM [3] is used to perform a multi-regionally coupled analysis of two-mixture flow and heat conduction in the reactor vessel considering the conjugate heat transfer on the solid-liquid interface. The internal fluid is two-component fluid, PCB and water, with different densities without chemical reaction. Advection equation for the volume fraction of two fluids, compressible Navier-Stokes equation with gravity term, and energy equation are staggeringly solved for unsteady thermal fluid analysis. The Reynolds-averaged Navier-Stokes equations based on the standard k-ε model are used for turbulent flow analysis. Temperature dependent thermo-physical properties of PCB and water such as specific heat, thermal conductivity and viscosity, and equation of state of density, are employed as polynomial equation of temperature. To evaluate the integrity of the hydrothermal oxidative destruction reactor vessel, corrosion risk was evaluated based on the results obtained from the analysis such as temperature, volume fraction of PCB and wall shear stress on the solid-liquid interface.

2 METHOD OF THE ANALYSIS AND EVALUATION OF CORROSION RISK

2.1 Governing equations

This study considers a two-mixture flow flow water and PCB based on the volume-of-fluid (VOF) method [4]. Volume fraction α_i of the fluid i (= 1,2) is defined as

$$\alpha_i = \frac{1}{V}\int_V X \, \mathrm{d}v \tag{4}$$

using a function $X(t,\boldsymbol{x})$ that takes 1 when the test volume V is occupied by each fluid and 0 otherwise at time t and location $\boldsymbol{x}$, note that $\alpha_1 + \alpha_2 = 1$. The behavior of volume fraction is obtained by solving the advection equation

$$\frac{\partial \alpha_i}{\partial t} + \nabla \cdot (\alpha_i \boldsymbol{u}_i) = 0 \tag{5}$$

where $\boldsymbol{u}_i$ is flow velocity vector of i-th fluid.

The equation of continuity, equation of motion, and equation of energy for an unsteady compressible two-fluid are respectively expressed as follows:

$$\frac{\partial}{\partial t}(\alpha_i \rho_i) + \nabla \cdot (\alpha_i \rho_i \boldsymbol{u}_i) = 0 \tag{6}$$

$$\frac{\partial}{\partial t}(\alpha_i \rho_i \boldsymbol{u}_i) + \nabla \cdot (\alpha_i \rho_i \boldsymbol{u}_i \boldsymbol{u}_i) = -\alpha_i \nabla p + \nabla \cdot (\alpha_i \boldsymbol{\tau}_i) + \alpha_i \rho_i \boldsymbol{g} + \sum_{j=1}^{2} M_{ij}\left(\boldsymbol{u}_j - \boldsymbol{u}_i\right) \tag{7}$$

$$\frac{\partial}{\partial t}\left\{\alpha_i \rho_i (h_i + K_i)\right\} + \nabla \cdot \left\{\alpha_i \rho_i (h_i + K_i) \boldsymbol{u}_i\right\} = \nabla \cdot \left(\alpha_i \frac{\lambda_i}{c_{p_i}} \nabla T_i\right) + \alpha_i \frac{\partial p}{\partial t} + E_i \tag{8}$$

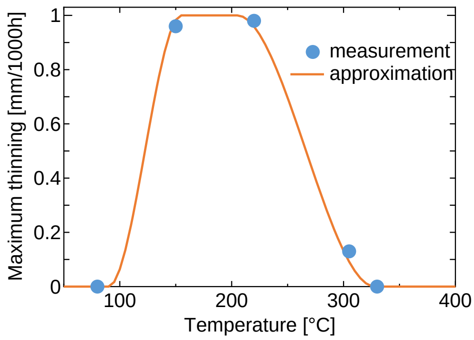

Figure 1: Corrosivity of Inconel NCF 690 with respect to temperature

where the subscript i denotes the i-th fluid, ρ_i is the density, p is pressure common to the two fluids, $\boldsymbol{\tau}_i$ is the stress tensor, $\boldsymbol{g}$ is the gravitational acceleration vector, M_{ij} is the mutual momentum transport between the fluids i, j such as drag and lift forces, h_i, K_i are the enthalpy per unit mass and kinetic energy, T_i is temperature, λ_i is thermal conductivity, c_{p_i} is specific heat at constant pressure, and E_i is mutual heat transfer between fluid i and other fluid.

The heat conduction equation in the solid region is as follow:

$$\frac{\partial T}{\partial t} = \frac{\lambda}{\rho c} \nabla^2 T \tag{9}$$

where λ, c, ρ are thermal conductivity, specific heat and density, respectively. At the solid-liquid interface, the fluid and solid temperature and heat flux continuity conditions are satisfied for Eqns. (8) and (9).

2.2 Method of corrosion risk evaluation

The corrosion risk r of the inner wall of the reactor is evaluated using three factors as follows: (1) temperature sensitivity of the reactor material (Inconel NCF 690) to corrosion based on experimental results, (2) PCB volume fraction, and (3) wall shear stress on the solid-liquid interface.

$$r = C_1 f(T) + C_2 \alpha_{\mathrm{PCB}} + C_3 \frac{||\boldsymbol{\tau}||}{\tau_{\max}} \tag{10}$$

where the first term on the right-hand side $f(T)$ is from the experimental results of measuring the maximum thinning of Inconel NCF 690 in NaCl, Na_2CO_3, CO_2 and O_2 dissolved in water at high pressure 26.5 MPa after 1000 h, the staircase function with temperature is approximated by a cubic equation, as shown in Fig. 1. Corrosion occurs in the temperature range of about 100 to 300 °C. The second term is the PCB volume fraction at the solid-liquid interface α_{PCB} obtained by the analysis. The third term normalizes the norm of wall shear stress

$$\boldsymbol{\tau} = -\boldsymbol{n} \cdot \mu \left\{ \nabla \boldsymbol{u} + \nabla \boldsymbol{u}^{\mathrm{T}} - \frac{2}{3} (\nabla \cdot \boldsymbol{u}) \boldsymbol{I} \right\} \tag{11}$$

at the solid-liquid interface by the maximum value $\tau_{\max}$.

C_1 to C_3 are the weight coefficients for each corrosion factor, where $C_1 = C_2 = 0.4, C_3 = 0.2$. The evaluated values of the three corrosion factors are $0 \le f(T), \alpha_{\mathrm{PCB}}, ||\boldsymbol{\tau}||/\tau_{\max} \le 1$ and $\sum_{i=1}^{3} C_i = 1$, thus corrosion risk is evaluated in the $0 \le r \le 1$ range.

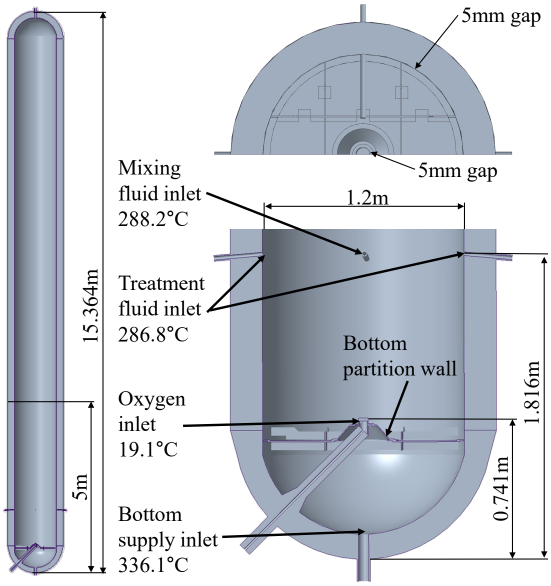

Figure 2: Three-dimensional solid model of hydrothermal destruction reactor

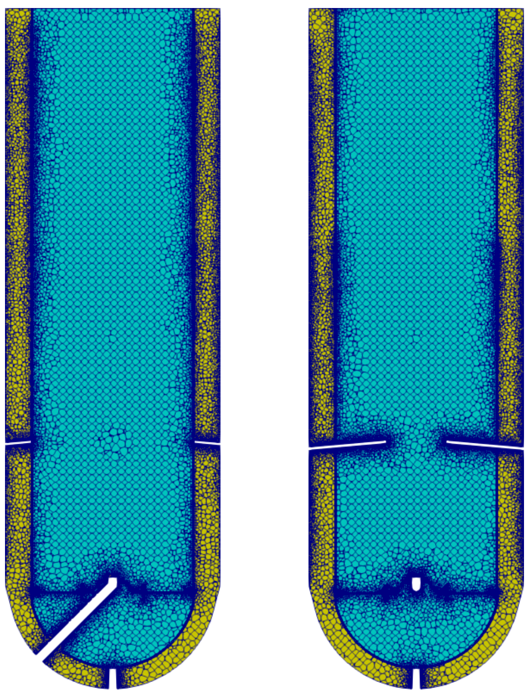

(a) Symmetry surface (b) Mixing pipe cross-section

Figure 3: Finite volume mesh

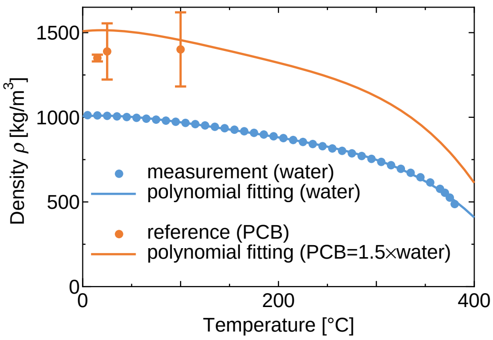

(a) Density

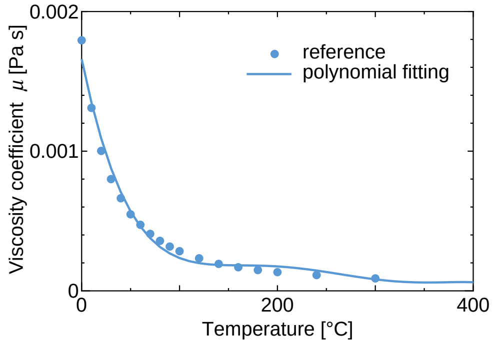

(b) Viscosity coefficient

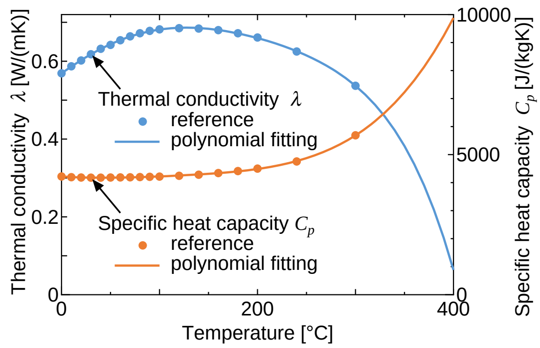

(c) Thermal conductivity and Specific heat capacity

Figure 4: Temperature dependent thermophysical properties of fluid

3 FINITE VOLUME MODEL AND ANALYSIS CONDITIONS

3.1 Construction of 3D finite volume model

In this study, 3-dimensional (3D) solid model shown in Fig. 2 was constructed using a 3D CAD software based on the configuration drawing of the actual reactor. Although there are various structure parts such as pressure sensing tubes inside the actual reactor, in this study, the analysis domain is from the bottom of the vessel to the height of 5 m in order to focus on the thermal flow phenomena at the bottom of the vessel.

Polyhedral unstructured FVA mesh is generated using a automatically meshing software ennova CFD for OpenFOAM [5] based on 3D geometry data in the standard triangulated language (STL) format of the 3D solid vessel models. Figure 3 shows FVA mesh. In the figure, yellow and light blue cells represent solid and fluid regions, respectively. The number of cells in the fluid and solid regions are 900109 and 538393 respectively, total number of cells is 1438502.

3.2 Thermophysical properties and boundary conditions

In order to express temperature dependence of the thermophysical properties of the internal fluid, density ρ [kg/m^3], viscosity μ [Pa s], thermal conductivity λ [W/(m K)], and specific heat c_p [J/(kg K)] are approximated by polynomial equations of temperature T [K],

$$f(T) = \sum_{i=0}^{N} a_i T^i \tag{12}$$

as shown in Fig. 4, where N is degree of the polynomial, $a_0, a_1, \ldots, a_N$ are coefficients and are calculated by least squares approximation. Literature values for the density of PCBs were only available for 15 °C, 25 °C, and 100 °C. The density of PCBs also depends on number of chlorines as shown in the orange error bars in Fig. 4(a). Therefore, the density of PCBs was set to 1.5 times that of water to provide a good approximation of the density of PCBs at around 100 °C. For the heat conduction analysis of the vessel body, temperature independent thermophysical properties of inconel (NCF690) are shown in Table 1.

Boundary conditions of multi-regionally coupled analysis are summarized in Table 2. At each inlet of the fluid region, temperature and flow velocity are set based on the measured values during actual operation of the reactor. Since the oxygen nozzle has a double circular structure and is constantly cooled by cooling water, temperature on the side wall of the nozzle is set to 19.1 °C. At the outlet, which is the top surface of the FV models, pressure is set to 26.5 MPa due to the measured value inside the actual vessel, and the uniform velocity outlet condition is configured. In addition, the outlet temperature is set to 369.9 °C, which is also the measured value, to simulate the heat generated by the chemical reaction in the hydrothermal oxidative decomposition of PCBs. On the outer wall of the vessel of solid region, heat transfer is insulated. The conjugate heat transfer is considered on the solid-liquid interface that are inner wall of vessel and surfaces of bottom partition.

At first, multi-regionally steady state analysis of single flow only water is performed to obtain initial conditions such as temperature, pressure and velocity for the unsteady multi-regionally two-flow analysis. And then, the multi-regionally unsteady analysis is performed when PCBs inflow from the mixing pipe to a steady flow of a single fluid containing only water into the reactor.

4 RESULTS AND DISCUSSIONS

The volume fraction distributions of the symmetrical surface of the reactor and the bottom of the reactor viewed from above after 30 s had elapsed since the start of PCB feeding are shown in Fig. 5. PCBs fed through the mixing tube settle out of the gap between the tip of the oxygen nozzle and the surrounding partition and are deposited on the bottom of the reactor. The PCB deposition on the bottom is reduced when the bottom water supply is high.

The distribution of temperatures $T = \sum_{i=1}^{2} T_i \alpha_i$ averaged over each temperature T_i of water and PCBs according to their volume fractions is shown in Fig. 6. The temperature at the bottom of the reactor is lowered by cooling with oxygen nozzle. However, the temperature at the bottom of the partition rises as the bottom feedwater volume increases. The temperature distribution at the bottom of the reactor is also high due to the increase in the bottom feedwater volume.

The vertical velocity distribution is shown in Fig. 7. The increase in the bottom feedwater flow rate shows that the upward flow from the bottom feedwater inlet blocks the downward flow cooled by the oxygen nozzles.

The corrosion risk distribution at the bottom of the reactor is shown in Fig. 8. The red area with the highest risk value is the largest for 50 kg/h with a low bottom water supply. The corrosion risk value decreases with an increase in the bottom water supply because of the higher temperature at the bottom of the reactor and the decreasing in PCB deposition.

Table 1: Thermophysical properties of inconel alloy (NCF690, 20 °C)

Density ρ	8200 kg/m^3
Specific heat c_p	450 J/(kg K)
Thermal conductivity λ	12 W/(m K)

Table 2: Boundary conditions

	Fluid region				Solid region
	Temperature [°C]	Velocity [m/s]	Pressure [MPa]	PCB volume fraction [−]	Temperature [°C]
Mixing fluid inlet	288.2	0.6950		1	288.2
Side wall of mixing fluid nozzle	288.2	non-slip		zero-gradient	288.2
Treatment fluid inlet	286.8	0.6040		0	286.8
Side wall of treatment fluid nozzle	286.8	non-slip		zero-gradient	286.8
Oxygen inlet	19.1	0.0467		0	19.1
Side wall of oxygen nozzle	19.1	non-slip		zero-gradient	19.1
Bottom supply inlet	336.1	variable*		0	336.1
Outlet (top surface)	369.9	uniform	26.5	zero-gradient	369.9
Outer wall of vessel	—	—	—	—	insulation
Inner wall of vessel	heat transfer	non-slip		zero-gradient	heat transfer
Bottom partition	heat transfer	non-slip		zero-gradient	heat transfer

*Velocity at bottom supply,
50 kg/h = 0.0074 m/s, 119 kg/h = 0.0176 m/s, 177 kg/h = 0.0263 m/s, 240 kg/h = 0.0355 m/s.

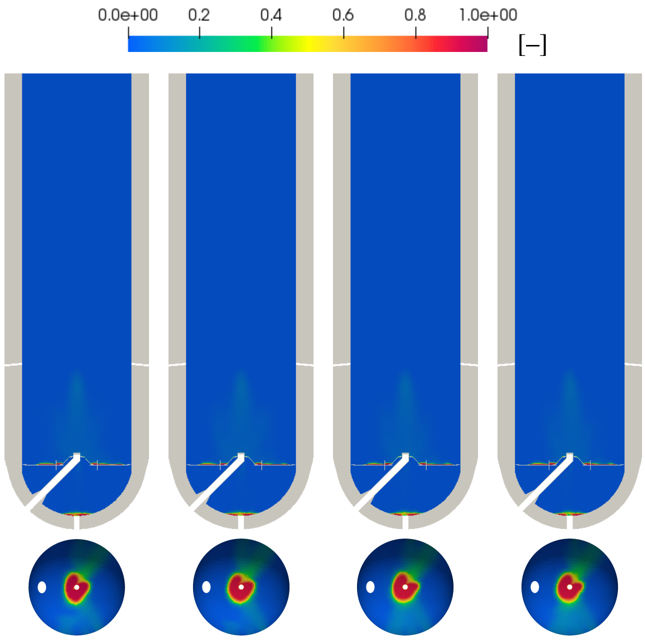

(a) 50 kg/h (b) 119 kg/h (c) 177 kg/h (d) 240 kg/h

Figure 5: PCB volume fraction distribution

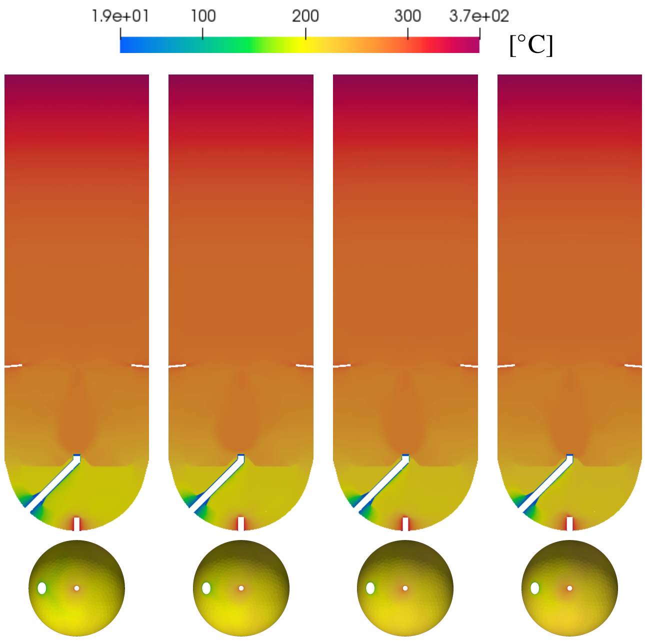

(a) 50 kg/h (b) 119 kg/h (c) 177 kg/h (d) 240 kg/h

Figure 6: Temperature distribution

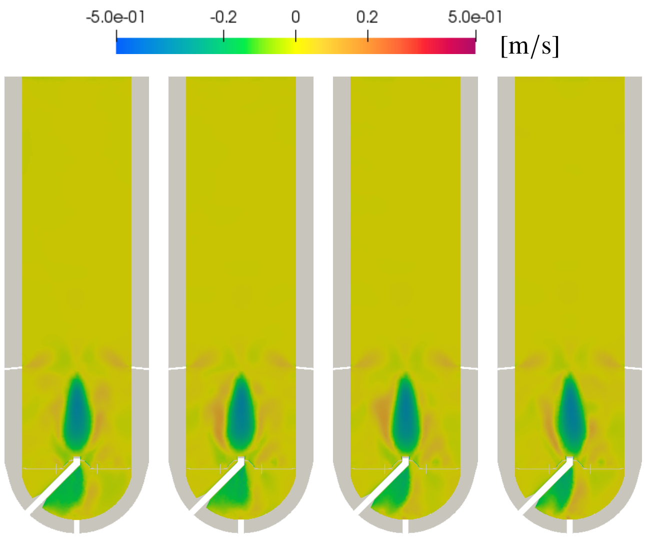

(a) 50 kg/h (b) 119 kg/h (c) 177 kg/h (d) 240 kg/h

Figure 7: Velocity distribution in the vertical direction

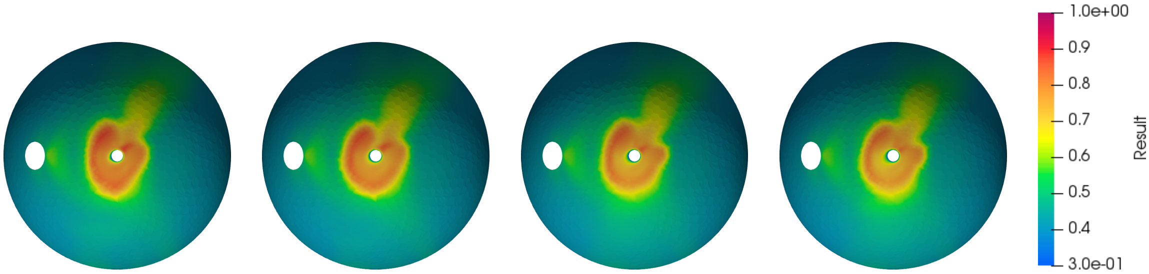

(a) 50 kg/h (b) 119 kg/h (c) 177 kg/h (d) 240 kg/h

Figure 8: Corrosion risk distribution

5 CONCLUSIONS

In this study, multi-regionally coupled analysis of thermal two-mixture flow and heat conduction analysis for the vessel body is performed for hydrothermal oxidative destruction reactor of PCBs. From the analysis results, a method for evaluating corrosion risk was proposed, and it was suggested that corrosion risk could be reduced by increasing the bottom water supply.

ACKNOWLEDGMENT

The authors would like to acknowledge providing actual data of the hydrothermal oxidative destruction reactors and the financial support of the Tokyo PCB Waste Treatment Facility, Japan Environmental Storage & Safety Corporation (JESCO).

REFERENCES

[1] Sugimoto, T., Kuramae, H., Matsumoto, M. and Watanabe, N. Thermal Fluid Coupled Analysis of Hydrothermal Destruction Reactor, *14th World Congress of Computational Mechanics and ECCOMAS Congress 2020*, (2021), **1200**.

[2] Maeda, T., Ueda, K., Fukusumi, T., Shinoda K. and Tateishi, M. Treatment of PCB by Hydrothermal Decomposition. *Mitsubishi Heavy Industries Technical Review*, (2001) **38**-1: 32–35 (in Japanese).

[3] OpenFOAM, `https://www.openfoam.com/`

[4] Prosperetti, A. and Tryggvason, G. *Computational Methods for Multiphase Flow*. Cambridge, (2009).

[5] IDAJ: ennovaCFD for OpenFOAM. `https://www.idaj.co.jp/product/ennovacfd/openfoam_gui/`.